An Adaptive Phasor Estimator for Power System Waveforms Containing Transients

Jinfeng Ren, *Student Member, IEEE*, and Mladen Kezunovic, *Fellow, IEEE*

***Abstract*—Synchronized phasor measurement has gained wide acceptance in many power system applications, particularly for tracking dynamic transitions during various disturbances. Fourier filter-based phasor estimation algorithms, which have been predominately used in phasor measurement units, have difficulties in processing dynamic sinusoidal waveform distortions, such as modulation, frequency drift, abrupt change in magnitude, etc. This paper proposes an adaptive approach for accurately estimating phasors while eliminating the effect of various transient disturbances on voltages and currents. The method preanalyzes the waveform spanning the window of observation to identify and localize the discontinuities which affect the accuracy of phasor computation. A quadratic polynomial signal model is used to improve the accuracy of phasor estimates during power oscillations. Extensive experimental results demonstrate the advantages. The method was implemented on a PC-based PXI system for real-time phasor computations. It can also be used as reference algorithm for testing the performance of the devices extracting synchronized phasor measurements.**

***Index Terms*—Abrupt step changes, amplitude modulation (AM), phase modulation, phasor estimation, phasor measurement, power system transients, wavelet transforms.**

I. Introduction

NEW applications using synchronized phasor measurements for enhancing the power grid reliability and security become an important part of the overall smart-grid deployment [1], [2]. The examples, such as real-time dynamic state monitoring, state estimation, model validation, and instability detection/islanding are improving wide-area visualization, protection, and control [3]–[11]. The accuracy of phasor measurements becomes an essential aspect that may directly affect the application performance and, hence, may have a profound impact on the entire system.

As defined by Steinmetz [12], a static sinusoidal waveform with known frequency can be represented by its amplitude and angular position with respect to an arbitrary time reference. The Fourier filter, which is widely used in phasor measurement units (PMUs), can accurately compute phasors for the signals with constant parameters within an observation interval. IEEE C37.118-2005 standard defines the synchrophasor measurements used in power system applications and specifies the performance requirements under steady-state conditions [13]. In general, power system voltage and current waveforms are not static sinusoids. Instead, they contain sustained harmonics and noise. During system disturbances, oscillations, step changes, and high-frequency interference in the magnitude and phase angle may occur because of the faults, switching operations, and electromechanical transients of machine rotors. The Fourier-based phasor estimation algorithms are derived based on the static sinusoidal signal model [14]. As a result, significant algorithm errors are expected when dynamic waveforms containing modulation, an abrupt change in magnitude and/or phase angle, and frequency drifts are used as inputs.

The Power System Relaying Committee (PSRC) is updating the synchrophasor standards with a specification of dynamic requirements for PMUs. This will accelerate the applications in power systems and enhance the interoperability for products from different vendors. Meanwhile, many efforts have been made to improve the accuracy of phasors' computation under transient conditions.

A raised cosine filter is proposed in [15]. This filter is able to obtain accurate results during amplitude modulation. An intuitive way to improve the estimates for signal oscillation is to use the polynomial models in magnitude and phase angle, instead of constant values, and then to approximate the envelope of the changing waveform parameters within an observation span. Based on this idea, paper [16] proposes a second-order Taylor polynomial model to improve the measurements under power system oscillations. If the parameters reflecting the changing characteristics of signals can be estimated, this provides more information to the applications tracking the dynamic progress compared to the traditional static phasor. Papers [17] and [18] define the dynamic phasor computation using multiparameter models and provide a compensation method for canceling the error in the classical Fourier algorithm that arises under dynamic conditions. Some issues regarding implementation of the algorithm in different intelligent electronic devices (IEDs) are discussed as well.

In [19], the phasor measurements under transient system conditions are reviewed looking at the basic definition, estimation architecture, and power system dynamic characteristics. As discussed in [19], step changes in the magnitude and phase angle because of electromagnetic transients may occur within the computation data window, in which case, the phasor estimate obtained from that window may be invalid. This may

Manuscript received March 20, 2011; revised September 14, 2011; accepted January 07, 2012. Date of publication February 23, 2012; date of current version March 28, 2012. This work was supported by National Science Foundationn I/UCRC called Power System Engineering Research Center (PSERC) under the Project T-43 titled "Verifying Interoperability and Application Performance of PMUs and PMU-enabled IEDs at the Device and System Level." Paper no. TPWRD-00235-2011.

The authors are with the Department of Electrical and Computer Engineering, Texas A&M University, College Station, TX 77843-3128 USA (e-mail: j.f.ren@neo.tamu.edu; kezunov@ece.tamu.edu).

Color versions of one or more of the figures in this paper are available online at http://ieeexplore.ieee.org.

Digital Object Identifier 10.1109/TPWRD.2012.2183896

postpone the response time of the time-critical applications, and in the worse cast, it may cause wrong protective or control decisions. How to properly solve this issue is not addressed in the aforementioned efforts [15]–[19].

In this paper, the effect of power system transients on phasor behavior is analyzed in Section II. A wavelet method is used to preanalyze the waveform within an observation window in Section III. It can detect and localize various disturbances while discriminating the valid steps from noise. In Section IV, once a valid discontinuity is localized, an adaptive window containing valid data is used to fit a quadratic polynomial model in the sense of least square error. The signal model has perfect accuracy when representing the magnitude and phase-angle-modulated signals. The algorithm implementation and application studies are presented in Sections V and VI, respectively, and conclusions are outlined at the end.

II. Power System Transients

The power system suffers various disturbances all of the time. Relying on different types of control and protective functions, the system can remain in dynamic stable condition. Some disturbances, for example, faults and switching operations, produce discontinuous points, such as steps and ramps in voltage and current waveforms, respectively, due to electromagnetic transients. The effect of these transients also results in high-frequency components in voltage and current signals. Typically, the phasor measurements are calculated at a certain rate (i.e., reporting rate [13]), and phasor estimation is determined over one cycle of nominal power frequency. The discontinuities in waveforms caused by the transients may occur within an observing data window. In this case, the accuracy of the phasor output estimated over such a data window is affected by the discontinuities, and it can neither represent the pre-state nor the post-state accurately.

An example for computing the phasors representation of a waveform with an abrupt step in the amplitude and phase angle is given in Fig. 1. The step forms a boundary which separates the pre-disturbance from the post-disturbance segment. Assuming the observing window spans N samples, as the computation window moves forward when new samples are obtained, the data window k and $k+N$ are the windows closest to the boundary containing only the samples belonging to the pre-disturbance and post-disturbance, respectively. The phasors calculated through the windows $k+1$ to $k+N-1$ represent neither the pre- nor post-segments. Fig. 2 shows the phasors during the transition period. Use of such phasor estimates for any type of protection or control application may be inappropriate. A technique for identifying the discontinuities while eliminating their impact on the accuracy of outputs will be described later in this paper. The technique can also be used to flag such invalid phasor measurements.

A power swing may occur in a power system when a balance between the power generation and consumption is broken because of the fault, line switching, generation tripping, loss of load, or other system disturbances. This phenomenon in power systems can be categorized as the electromechanical transient

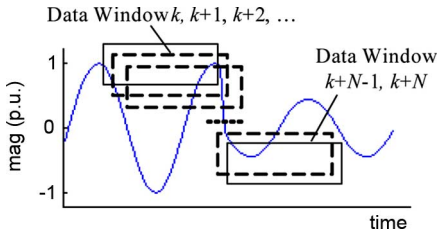

Fig. 1. Moving data windows for estimating a waveform with steps in amplitude and phase angle.

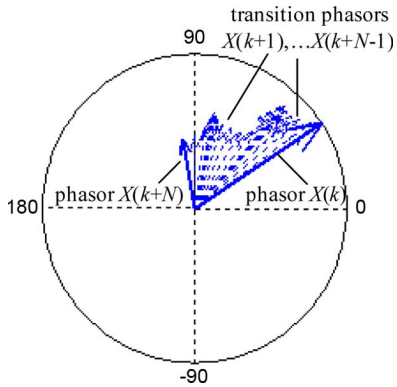

Fig. 2. Evolution of phasor measurements over the transient period.

because it typically involves the rotor movement of large electric machines. During the power swing, the amplitude and phase angle of the voltage and current are modulated with a low-frequency signal which corresponds to the deviation of rotating speed among generators. Various examples of power swings observed in practice can be found in technical reports [20]. Let us consider an example of oscillations caused by a three-phase fault. The waveform of phase-A voltage and its amplitude envelope are given in Fig. 3(a). The relay operation was delayed and the oscillation started after the fault was cleared. A discrete Fourier transform (DFT)-based algorithm is used to compute the phasors. This algorithm is the widely used technique in presently available PMUs though it has difficulty in dealing with sinusoids with changing parameters. Fig. 3 shows the dynamic behavior when the algorithm is exposed to the steps and modulations. The phase estimates and total vector error (TVE), which is defined in [13] is given in Fig. 3(b) and (c), respectively. In this example, the TVE reaches 2.6% during oscillation, which may hardly meet some applications requirements. The accuracy during the power swing needs to be improved.

III. Disturbance Identification and Localization

The step in a waveform discussed before is one class of edges, also know as singular points as called in mathematics, which exist among different segments of the waveform. In the area of image processing, the edges contain a lot of critical information and the detection of them plays a significant role in the discipline. Many techniques have been proposed to detect and further characterize the singularity of signals [21], [22]. This paper utilizes these principles and makes improvement for better resolving the specific problems raised in a power system.

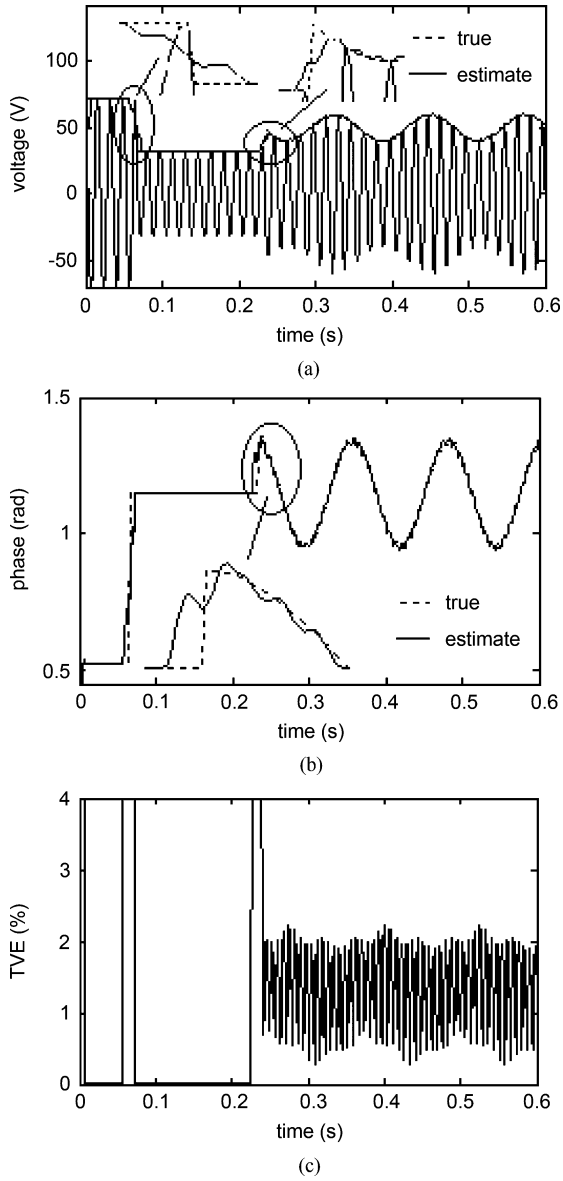

Fig. 3. Oscillation example and estimated phasors by the DFT-based algorithm. (a) Voltage waveform and amplitude estimate. (b) Phase angle estimate. (c) TVE.

A. Lipschitz Exponent

The local regularity of a function can be mathematically measured with Lipschitz Exponent α (i.e., LE α, which is defined as follows [21]).

Definition 1: A function $f(t)$ $t \in (c,d)$ is described to be Lipschitz α at point t_0, if a constant K and a polynomial $P_n(t)$ exist so that $\forall t_0 \in (c,d)$, and the following is held:

$$|f(t) - P_n(t)| \leq K|t - t_0|^{\alpha}. \tag{1}$$

Based on the above definition, one can easily prove that for a positive integer n, if $f(t)$ is LE $\alpha > n$, then $f(t)$ is n times differentiable at point t_0 while the polynomial $P_n(t)$ is the first $n+1$ terms of the Taylor series of $f(t)$ at t_0. LE indicates the differentiability of a function. Furthermore, if the LE α of $f(t)$ satisfies $n < \alpha < n+1$, then we learn that $f(t)$ is n times differentiable at t_0, but its nth derivative is singular at this point and the LE characterizes its regularity.

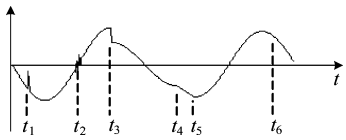

Fig. 4. Example of a sinusoidal waveform containing various components.

TABLE I
SPECIFIC FUNCTIONS AND THEIR LIPSCHITZ EXPONENTS

Location	Function	L. E.
t_1	Dirac (Impulse)	α = -1
t_2	White Noise	-1<α < -0.5
t_3	Step	α = 0
t_4, t_5	Ramp	α = 1
t_6	Sinusoidal	α >> 1

Fig. 4 shows a sinusoidal waveform containing some components, including noise, step edge, and ramp edge at different locations $(t_1, t_2, \ldots, t_5)$, which can be easily found in voltage and current measurements of the real power system. Mathematical functions, which represent these signal components and heir corresponding local Lipschitz regularities, are given in Table I. Ideally, the voltage and current waveforms are pure sinusoidal. They are usually contaminated by a variety of noise, among which the impulse noise and white noise are the two most common kinds. Sometimes step and ramp edges may occur in voltage and current waveforms due to the electromagnetic transients during faults and switch operations. From Table I, we know that the different functions can be discriminated with their LEs. The following sections will present the method for estimating the exponents approximately.

B. Wavelet Function and Transform Coefficient

The wavelet transform has proven to be an effective mathematical tool to analyze the regularity of a signal because of its remarkable capability of the localization in time and frequency domain. A wavelet is defined as a function $\psi(t) \in L^2(R)$ whose Fourier transform $\Psi(\omega)$ satisfies the admissibility condition

$$\int_{-\infty}^{+\infty} \frac{|\Psi(\omega)|^2}{|\omega|} d\omega = C_{\Psi} < \infty. \tag{2}$$

In time domain, this condition implies

$$\Psi(\omega)|_{\omega=0} = \int_{-\infty}^{+\infty} \psi(t)dt = 0. \tag{3}$$

Denote s and u as the scaling factor and time shifting factor, respectively. A set of wavelet functions can be derived by dilating and translating the mother wavelet $\psi(t)$

$$\psi_{u,s}(t) = s^{-1} \cdot \psi\left(\frac{t-u}{s}\right), \quad s > 0. \tag{4}$$

Definition 2: The wavelet transform of a function $f(t)$ with regard to time shift u and scale s is defined as

$$Wf(u,s) = f(t) * \psi^*_{u,s}(t) = s^{-1}\int_{-\infty}^{+\infty} f(t)\psi^*\left(\frac{t-u}{s}\right)dt \tag{5}$$

where $Wf(u,s)$ is denoted as the transform coefficient. Let the scale factor s change along the dyadic sequence of 2^j ($j = 1, 2\ldots$), and we have the dyadic wavelet function $\psi_{u,2j}(t)$ and its dyadic wavelet transform coefficient $Wf(u,2^j)$. For simplicity, we designate $Wf(u,j)$ for the rest of this paper.

It has been proven that the input signal can be perfectly reconstructed with the dyadic transform coefficient. Besides, it obtains efficient numerical implementations. The component of interest in the input signal, the singularity in this paper, can be exposed over the transform coefficient by selecting a proper wavelet and transform scales.

C. Measuring Signal Regularity With the Wavelet Transform

Assume the wavelet holds n vanishing moments (i.e., n times differentiable). That is, for all positive integer $k < n$, $\psi(t)$ satisfies

$$\int_{-\infty}^{+\infty} t^k\psi(t)dt = 0. \tag{6}$$

Theorem 1: Let n be a positive integer and $\alpha \le n$. If $f(t)$ is Lipschitz α at t_0, then a constant A exists so that for all point t in a neighborhood of t_0 and any scale s, the wavelet transform of $f(t)$ with regard to $\psi(t)$ (with n vanishing moments) holds

$$|Wf(u,s)| \le A(s^\alpha + |u-t_0|^\alpha). \tag{7}$$

Theorem 2: $f(t)$ and its wavelet transform is well defined over (c,d), and let $t_0\square(c,d)$. Suppose that a scale s_0 exists and a constant C, so that for $t\square(c,d)$ and $s < s_0$, all of the modulus maxima of $Wf(u,s)$, denoted as $Wf_{\max}(u,s)$, belong to a cone defined by

$$|t-t_0| \le C\cdot s. \tag{8}$$

Then, at all points, $t_1 \in (c,d)$, $t_1 \ne t_0$, and $f(t)$ is uniformly Lipschitz n in a neighborhood of t_1. Let $\alpha \le n$ be a non-integer. The function $f(t)$ is Lipschitz α at t_0, if and only if a constant A exists so that each modulus maxima is in the cone defined by (8)

$$|Wf_{\max}(u,s)| \le A\cdot s^\alpha. \tag{9}$$

The proof of the above theorems has been given by Mallat [21]. He pointed out that the maxima of the wavelet transform modulus can reflect the locations of the irregular structures. If we rewrite (9), then

$$\log_2\left(|Wf_{\max}(u,s)|\right) \le \log_2(A) + \alpha\log_2(s). \tag{10}$$

From (10), one can see that the Lipschitz regularity at point t_0 is the maxima slope of straight lines that remain above $\log_2(|Wf_{\max}(u,s)|)$ on a logarithmic scale s.

The dyadic wavelet transform ($s = 2^j$) for scale j and $j+1$ can be obtained from (10)

$$\log_2(|Wf_{\max}(u,j)|) \le \log_2(A) + \alpha\cdot j \tag{11}$$

$$\log_2(|Wf_{\max}(u,j+1)|) \le \log_2(A) + \alpha\cdot(j+1). \tag{12}$$

Subtracting (12) from (11), the LE α can be approximately estimated by the following equation:

$$\alpha \cong \log_2\frac{|Wf_{\max}(u,j+1)|}{|Wf_{\max}(u,j)|}. \tag{13}$$

Equation (13) shows that the Lipschitz α of a signal at any point can be approximately estimated by its modulus maxima of the dyadic wavelet transform over adjacent scales. Based on LE, one can identify the types of singularities. For example, if $|Wf_{\max}(u,j+1)| = |Wf_{\max}(u,j)|$ (i.e., $\alpha = 0$) it implies the signal is discontinuous at this point, such as step change; if $|Wf_{\max}(u,j+1)| < |Wf_{\max}(u,j)|$ (i.e., $\alpha < 0$), it implies that the signal is more singular than discontinuity at this point, such as Dirac and white noise; if $|Wf_{\max}(u,j+1)| > |Wf_{\max}(u,j)|$ (i.e., $\alpha > 0$), it means the signal is at least continuous such as a ramp, or smooth such as sinusoid.

D. Modulus Maxima Detection and Localization

In mathematics, the inflection points of a function correspond to the local extrema of the first derivative of the function or to the zero crossings of the second derivative of the function. Based on this, Canny developed a computational approach for edge detection using smooth functions [23].

Let f be the original signal and F be the smoothed one by function θ; for example, the Gaussian function whose integral is equal to one and it converges to 0 at infinity. In the sense of filtering $F = f*\theta$, where $*$ stands for the convolution operator. Suppose that θ is twice differentiable and define ψ and ψ' as the first- and second-order derivative of θ, respectively. In this case, the detection of edges is equivalent to locating the inflection points of the smoothed F, that is, to find the local extrema of $f*\psi$ or zero crossings of $f*\psi'$. Both local extremum and zero crossing give location information of the inflection point and detecting them is a similar procedure. However the local extremum approach has some important advantages. An inflection point of F can either be a maximum or a minimum of the absolute value of $f*\psi$. The maximum is a sharp variation point of F, which is the point of interest, whereas the minimum corresponds to slow variation. With a second derivative operator ψ', it is difficult to distinguish these two types of zero crossings. On the contrary, with the first derivative ψ, one can easily detect the sharp variation points by only locating the local maxima of $|f*\psi|$, which is the modulus of $f*\psi$. Besides, finding a maximum point is much easier than locating a zero crossing point.

In the frequency domain, the smooth function θ features a low-pass filter while its first derivative ψ is a band-pass filter. The function ψ can be considered to be a wavelet because its integral is equal to zero by definition. Let ψ_s be the function dilated by scale factor s. The wavelet transform of f under scale s is given by

$$Wf(s) = f*\psi_s. \tag{14}$$

From the above discussion, we know that the inflection points with sharp variations can be detected and localized by the modulus maxima of the wavelet transform.

E. Step Identification With LE

After detecting the disturbance points, one needs to further identify their types because the sharp variations may either be step or noise. As we discussed the types, regularities in mathematical terms can be characterized by LE which can be estimated by the evolution across scales of the wavelet transform modulus maxima $|Wf_{\max}(u,j)|$.

To achieve this goal, we construct a cubic order B-Spline function as the smooth function and its first-order derivative as the wavelet function (i.e., a quadratic B-Spline wavelet). This wavelet possesses desirable properties, such as the compact support, symmetry, and biorthogonality [24]. It has a simple analytical form in the frequency domain. The filter length for scaling function and wavelet function are 4 and 2, respectively. This feature results in an efficient numerical implementation for the multi-scale decompositions. For example, if one performs wavelet transform in two scales, $12N$ multiplications and summations will be required, where N is the length of input data.

In Fig. 5, four types of singularities—Dirac, white noise, step, and ramp are shown in (a) designated as p1–p4, respectively. Their transform coefficients of quadratic B-Spline wavelet from scale 1 to 3 are given in (b)–(c). From Fig. 5, we can observe that for the Dirac and white noise, the maxima of wavelet transform coefficient decrease along the evolution of scales while for the step and ramp, they increase along the evolution of scales. This can be clearly seen by the ratios of the wavelet transform modulus maxima for adjacent scales given in Table II, where $|Wf_{\max}(j)|$ stands for the modulus maximum under scale j. The LE estimates by (13) are given as well. It should be pointed out that magnitude steps in voltage and current waveforms are usually smoothed to appear as a ramp due to their traveling along the transmission lines. As a result, the LE will fall into the range between 0 and 1. For simplicity, let us designate such singularities as steps for the rest of this paper.

F. Implementation and Threshold

Let $f(k)$ be the samples of the input signal and N be the length of the observing data window. Suppose $f(k)$ is properly processed using the low-pass filter to comply with the Sampling Theorem. The process of disturbance detection will be performed to each observing data window (denoted as $f_{\mathrm{N}}(k)$) before directly estimating the phasor over it. The implementation procedure for disturbance detection is as follows.

1) Detect the singularity of the input signal to see if any disturbance occurs within this window span. Perform wavelet transform using the quadratic B-Spline wavelet in scale 1 to obtain the coefficient $Wf(k,1)(k = 1,2\ldots N)$. Under normal conditions, the signal is sinusoidal; thus, the coefficient $Wf(k,1)$ has no local modulus maxima. If there is no modulus maximum, the process is terminated and data will be handed over to the next process, such as phasor estimation; If the modulus maxima $Wf_{\max}(k,1)$ exist, then there are singularities within the window and locations can be found by $Wf_{\max}(k,1)$ as well.
2) Identify the type of singularities. The singularities can be either the real transient disturbances (abrupt steps) or the noise caused by a variety of interferences brought into the measurements. To further distinguish them, the wavelet transform coefficients in scale 2 are computed, and the modulus maxima $Wf_{\max}(k,2)$ are found.

If $|Wf_{\max}(k,2)|/|Wf_{\max}(k,1)| \geq 2^{\alpha=0} = 1$, the singularity is a step, and the data will be turned over to the process of the step handler.

If $|Wf_{\max}(k,2)|/|Wf_{\max}(k,1)| < 2^{\alpha=0.5} = 0.707$, the singularity is a noise; then, the process is terminated and data are turned over to the process for phasor estimation.

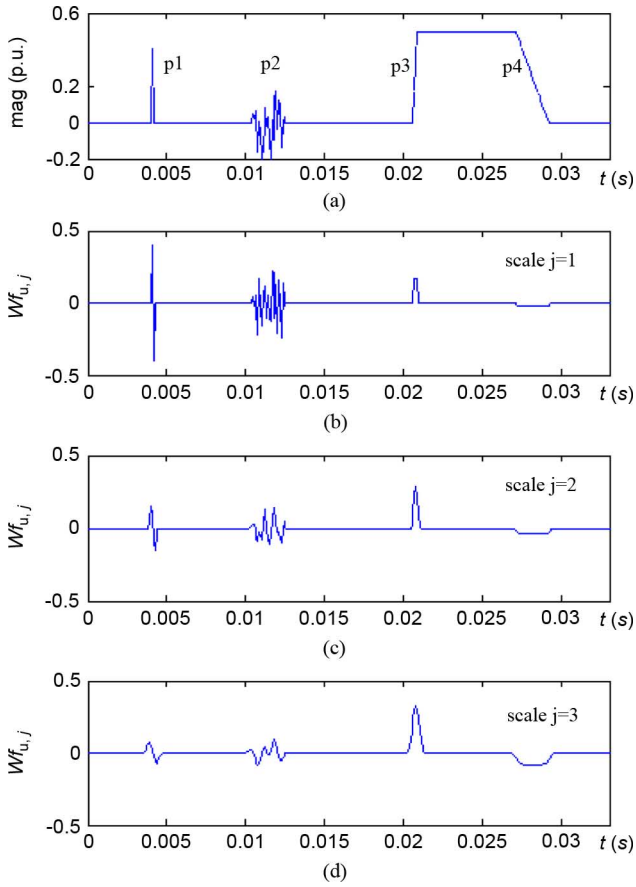

Fig. 5. Singularities and their coefficients of wavelet transform across scales.

TABLE II
RATIOS OF THE WAVELET TRANSFORM MODULUS MAXIMA AND LES.

Type	$\lvert Wf_{\max}(2)\rvert / \lvert Wf_{\max}(1)\rvert$	$\lvert Wf_{\max}(3)\rvert / \lvert Wf_{\max}(2)\rvert$	LE α
p1	0.38	0.45	-1.42/-1.12
P2	0.21	0.33	-2.26/-1.58
P3	1.75	1.11	0.81/0.15
P4	2.00	2.00	1.00/1.00

IV. ADAPTIVE SCHEME FOR PHASOR ESTIMATION

Typically, PMUs generate synchrophasors at submultiples of the nominal power system frequency. One cycle period of the input signal is commonly used as the length of the data window

Fig. 6. Adaptive phasor estimation approach.

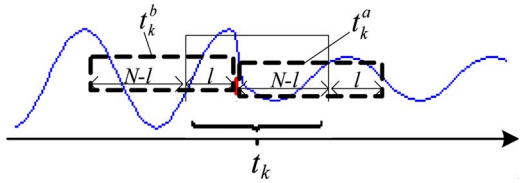

Fig. 7. Occurrence of a step change in a data window.

for phasor computations. The samples of voltages and currents in a window span are obtained at the same rate as the output phasors. And the position of window is either centered or sided (at the beginning or the end) at fixed points corresponding to timestamps. The abrupt steps in input signals may affect the accuracy of phasor outputs, particularly when the data window crosses the step point. This paper proposes an adaptive phasor estimation approach for achieving accurate phasor measurement under transients. As shown in Fig. 6, the approach consists of identifying disturbance, applying adaptive window, and implementing a new phasor estimation algorithm. The technique for detecting the transient disturbances has been discussed. This section will introduce an adaptive data window for avoiding or minimizing the impact of disturbances and presents a signal model for accurately estimating phasors during transients.

A. Adaptive Data Window

Suppose that the occurrence of a step change within a span of data window has been identified and localized. Let N be the length of the window. As shown in Fig. 7, the window for time stamp t_k (denoted as window t_k) contains a step change in waveform. The phasor computed over this window will represent neither the past (normal) state nor the present (faulty) state because it contains partial samples of both states. Since the position of the step change within this window has been estimated, we can use the data either before or after the step point.

To use the data before the singular point, the partial data with the length of l in window t_k, combining the data with the length of $N-l$, which is usually stored in a buffer with continuous sampling, forms the window t_k^b. It should be pointed out that the amplitude of the phasor estimated over the window t_k^b represents the past state while the phase angle starts showing the transition due to the selection of angle reference.

To use these data after the singular point window, t_k^a is formed by the partial data with the length of $N-l$ in window t_k combing the data with the length of l in the next sampling window. In this case, the amplitude and phase angle will represent the present state. The phasor output will be delayed because of the wait due to acquiring data l in the next sampling window.

Which data window will be used in the algorithm can be determined by the specific requirements of the applications. For example, some applications that require the least output latency may use the window t_k^b; some applications that require a rapid detection of the disturbance state, but can tolerate the delay to a certain level, may use the window t_k^a. How to select the data window for a specific application will not be discussed in this paper. Nevertheless, a simple rule will be followed and it will be used in the algorithm for the rest of this paper: if the singular point occurs in the first half of the window, as shown in Fig. 7, window t_k^a will be used for computing the phasor; if the singular point occurs in the second half of the window, window t_k^b will be used. Based on this rule, the maximum delay for using window t_k^a will be a half cycle (i.e., $N/2$ times the sampling interval).

B. Phasor Estimation Algorithm

The conventional DFT-based algorithms usually assume a sinusoidal signal model with constant amplitude and phase angle over the observation window. This assumption is not very rigorous for the signals during power system transients. For better describing the signal in transient state, a model with changing amplitude and phase angle is employed

$$y(t) = a(t) \cdot \cos[2\pi f_0 t + \varphi(t)] \tag{15}$$

where f_0 is the nominal frequency, and the amplitude $a(t)$ and phase angle $\varphi(t)$ are functions of time. Rewrite (15) as

$$y(t) = a(t) \cdot \cos[\varphi(t)] \cos(2\pi f_0 t) - a(t) \cdot \sin[\varphi(t)] \sin(2\pi f_0 t). \tag{16}$$

For an observation interval, the $a(t)\cos[\varphi(t)]$ and $-a(t)\sin[\varphi(t)]$ are the envelopes of the nominal frequency components $\cos(2\pi f_0 t)$ and $\sin(2\pi f_0 t)$, respectively. Using the quadratic expansion to approach the envelopes spanning the observation interval, we have

$$y(t) = (q_0 + q_1 t + q_2 t^2) \cdot \cos(2\pi f_0 t) - (r_0 + r_1 t + r_2 t^2) \cdot \sin(2\pi f_0 t) \tag{17}$$

where q_0, q_1, q_2, r_0, r_1, and r_2 are the coefficients of quadratic form.

According to the synchrophasor standard [13], the amplitude A_1 and phase angle φ_1 are computed over the observation window at the timestamp t_k, which is the point $t = 0$ in the window. This is also the reference point for computing the phase angle. From (15), we have $A_1 = a(t)|_{t=0}$, $\varphi_1 = \varphi(t)|_{t=0}$.

Let $\theta(t) = 2\pi f_0 t + \varphi(t)$, then the frequency at the reference point can be represented with

$$f_1 = \left.\frac{d\theta(t)}{2\pi dt}\right|_{t=0} = f_0 + \left.\frac{\varphi'(t)}{2\pi}\right|_{t=0}. \tag{18}$$

Estimating the quadratic coefficients in (17) can be achieved by resolving the linear regression problem. Suppose that the solution depends linearly on the data $\sum_j^M \gamma_{ij} x_j = y_i (i = 1, 2 \ldots N)$, that is, N linear equations in M, unknown coefficients $x_1, x_2, \ldots x_M$, with $N > M$. Rewrite this in matrix form as $H \cdot X = Y$. The fitting variables X are determined in the

least square error sense by solving the quadratic minimization problem $\arg\min \|Y - H \cdot X\|^2$.

For (17), the H matrix is $H = [\cos(2\pi f_0 t_i) - \sin(2\pi f_0 t_i) t_i \cos(2\pi f_0 t_i) - t_i \sin(2\pi f_0 t_i) t_i^2 \cos(2\pi f_0 t_i) - t_i^2 \sin(2\pi f_0 t_i)], (i = 1, 2 \ldots N)$. The corresponding fitting variable X vector is $X = [q_0 r_0 q_1 r_1 q_2 r_2]^T$, where T stands for the transpose. For a N-sample window, the H matrix is a $N \times 6$ matrix while the fit data Y is a $N \times 1$ vector. The position of the phase reference in a given observation window can be determined by assigning time vector $\overline{t}$. If the timestamp is located in the center of the window, let $\overline{t} = [-t_{N/2-1}, \ldots, 0, \ldots t_{N/2}]$; if the timestamp is located at the beginning or the end of the window, assign $\overline{t} = [0, t_1, \ldots t_{N-1}]$ or $\overline{t} = [-t_{N-1}, \ldots t_1, 0]$, respectively.

After obtaining the fit coefficients, the amplitude and phase angle over the observation window can be computed by the following equations:

$$A_1 = (q_0^2 + r_0^2)^{1/2} \tag{19a}$$

$$\varphi_1 = \arctan\left(\frac{r_0}{q_0}\right) \tag{19b}$$

$$f_1 = f_0 + \frac{q_0 r_1 - r_0 q_1}{2\pi(q_0^2 + r_0^2)}. \tag{19c}$$

And the rate of change of frequency $R_f = df_1/dt$. The derivation of the above equations is given in the Appendix.

C. Model Accuracy Studies

Equation (17) uses the quadratic form to approach the envelope of the slow changing in an observation interval. The adequacy of such approximation is investigated to ensure the model is capable of representing the voltage and current signals measured from the real system. The new synchrophasor standard C37.118.1-2011 defines dynamic signal models and corresponding specification requirements [25]. This paper uses the signal models and test conditions defined in the standard draft to study the accuracy of a phasor estimation algorithm.

Two types of signals representing the power oscillation and frequency ramp are given as follows.

D. Power Oscillation

$$y_1(t) = A_m[1 + k_x \cos(2\pi f_m t)] \cdot \cos[2\pi f_0 t + k_a \cos(2\pi f_m t - \pi)] \tag{20}$$

where A_m is the constant amplitude, f_m is the modulation frequency, and k_x and k_a are the modulation factors for amplitude and phase angle, respectively.

E. Frequency Ramp

$$y_2(t) = A_m \cos(2\pi f_0 t + \pi f_d t^2 + \varphi) \tag{21}$$

where f_d is the rate of frequency change and φ is the initial phase.

TABLE III
RESULTS FOR ACCURACY STUDIES

Type	Conditions (100% rated magnitude and f_0 at start)	Max TVE (%)	Max $\lvert\Delta f\rvert$ (Hz)
a	f_m: 0.1 Hz to 12 Hz k_x: 0 to 0.2, k_a: 0 to 0.2.	0.028	0.046
b	f_d: ±0.1 Hz to ±1 Hz Ramp range: ±5 Hz	0.032	0.026

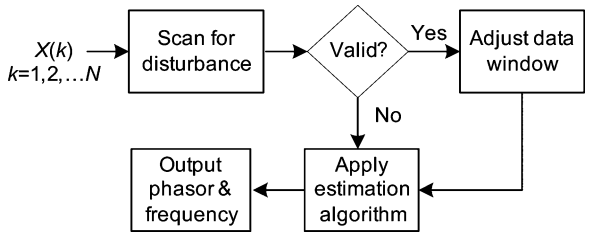

Fig. 8. Implementation flowchart for the adaptive approach.

0.1% white noise (SNR 60 dB) is added to the test signals. We use one cycle as the observation interval for the phasor measurement. The TVE and the frequency error Δf are used to measure the estimation accuracy. Abundant scenarios that may be observed in the real system are studied as summarized in Table III. The test conditions are more severe than these required by the standard.

Due to the limited space in this paper, only the maximum value of TVE and frequency error, which correspond to the most rigorous conditions, are given in Table III. For example, as related to type "*a*," the most rigorous condition is $f_{\rm m} = 12$ Hz, $k_x = k_a = 0.2$. The typical TVE and frequency error are at the level of 0.01% and 1 MHz, respectively. The results demonstrate that the model approach is adequate for representing the power signal under transient conditions.

V. IMPLEMENTATION

The adaptive phasor estimation approach has been implemented for real-time use in the synchrophasor measurement test system, which was developed on a PC-based PXI platform (by National Instruments) and used for PMU calibration and testing [26]. The system consists of a controller, time synchronization clock, and data acquisition modules. It is capable of performing synchronous sampling for eight channels at up to 500 kHz. The implementation flowchart of the adaptive scheme is shown in Fig. 8, where the "valid" means that the input samples within the observation window have discontinuity caused by electromagnetic disturbance instead of noise.

Solving the quadratic minimization problem $\arg\min \|Y - H \cdot X\|^2$ is equivalent to solving $\partial \|Y - HX\|^2 / \partial X = 0$, That is

$$-2H^T(Y - HX) = 0. \tag{22}$$

Let's designate $H^T \cdot Y$ as Z, and $H^T \cdot H$ as G. If we rewrite (22), we have

$$G \cdot X = Z \tag{23}$$

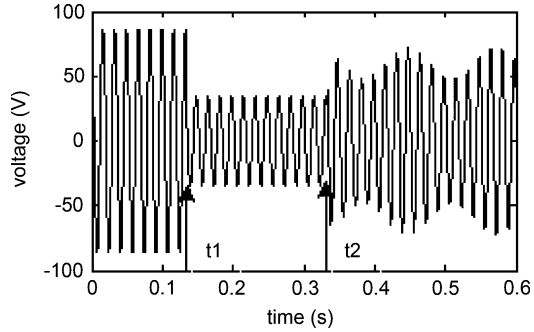

Fig. 9. Voltage waveform under fault and power swing conditions.

where G is a 6×6 matrix, and Z is a 6×1 vector. Then, the fitting variables X can be estimated by solving (23). For efficient implementation, the coefficient matrix G can be calculated in advance and decomposed into LU matrices for fast computation. It has been proven that the matrix G is nonsingular.

For a given size of data window N, the disturbance check requires about $12N$ multiplications and summations while phasor estimation requires $6N + 30$ multiplications and $6N + 20$ summations. The computational burden is very low. We have demonstrated that the adaptive approach can be realized in real-time.

VI. Application Studies

We use voltages and currents generated from the time domain program Alternate Transients Program (ATP)/Electromagnetic Transients Program (EMTP) to evaluate the performance of the adaptive phasor estimator under transient conditions. The power system model is a 230 kV power network created by IEEE Power Engineering Society's Power System Relaying Committee (PSRC) [27]. The files recording voltage and current waveforms are read by the program and fed to algorithms. Two scenarios are considered: one is a transmission-line fault followed by tripping of faulted line that caused a power swing; another is an out of step due to a loss of load. We use 1.92 kHz sampling frequency and one cycle data window. For better illustrating the relationship between amplitude estimates and input waveforms, the peak value instead of the rms value is used. The estimates from three algorithms are compared: the adaptive phasor estimator (denoted as APE), the DFT-based algorithm, and the four-parameter algorithm (denoted as FPA) in [17].

A. Power Swing After Three-Phase Fault

We use one phase voltage (from the secondary side of the instrument transformer) as the input fed to the phasor estimation algorithms. As shown in Fig. 9, two disturbances occurred at t_1 and t_2 which stand for the three phase fault and the clearance of fault, respectively, and oscillations followed. The estimated amplitude, phase angle, frequency, and TVE in the vicinity of t_1 and t_2 for the three algorithms are given, respectively, in Figs. 10–13 at an appropriate zoom. One can see that the DFT and FPA suffer step effects when exposed to the disturbances, particularly for the frequency estimation. In Fig. 13, the TVEs exceed 10% during transitions. The proposed method is capable of detecting the disturbances and computing phasors with adaptive windows. In this case, the phasor estimates can follow the input changes very well. The maximum TVEs for DFT, FPA, and APE during oscillation are 2.42%, 0.89%, and 0.12%, respectively.

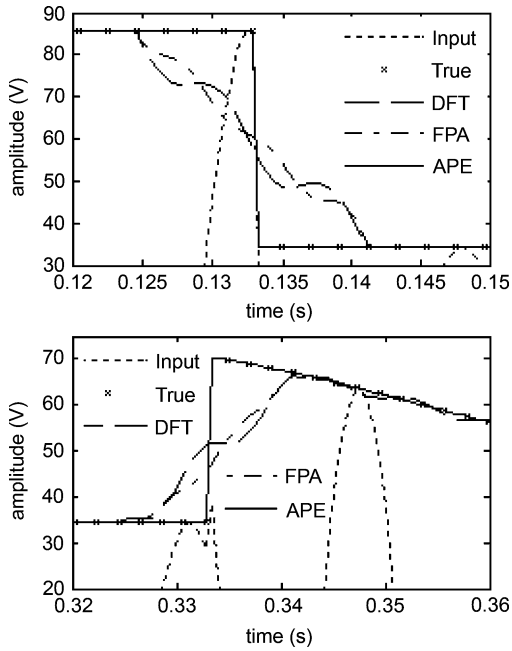

Fig. 10. Amplitude estimates of three algorithms at t_1 and t_2.

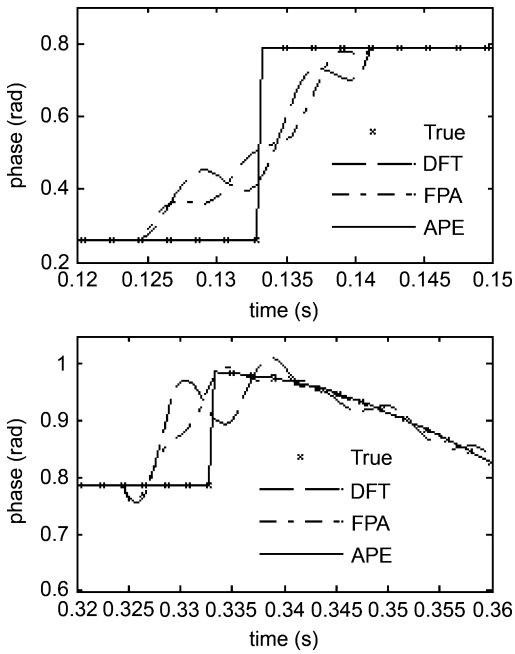

Fig. 11. Phase estimates of three algorithms at t_1 and t_2.

B. Out of Step Caused by Loss of Load

One phase current (from the secondary side of the instrument transformer) is fed to the phasor estimation algorithms.

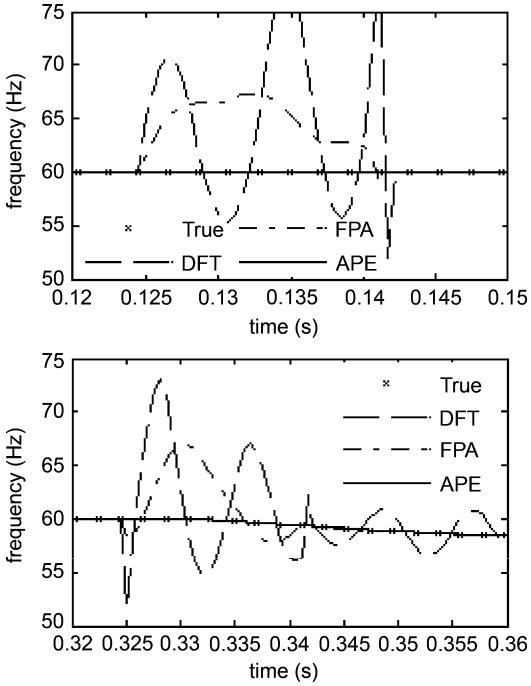

Fig. 12. Frequency estimates of three algorithms at t_1 and t_2.

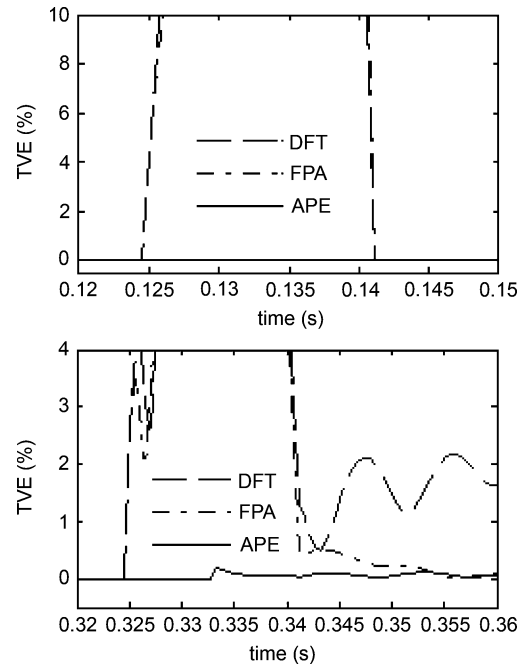

Fig. 13. TVE of three algorithms at t_1 and t_2.

Fig. 14 shows the current waveform measured during disturbances. The estimated amplitude, phase angle, frequency, and TVE by the three algorithms are given in Fig. 15. Compared to the DFT-based algorithm, both the four-parameter algorithm and the proposed phasor estimation method can follow the input during oscillations. The maximum TVEs for DFT, FPA, and APE after t_2 are 4.2%, 1.3%, and 0.086%, respectively. This proves that the proposed dynamic phasor model achieves better accuracy than that of the four-parameter model. From the TVE

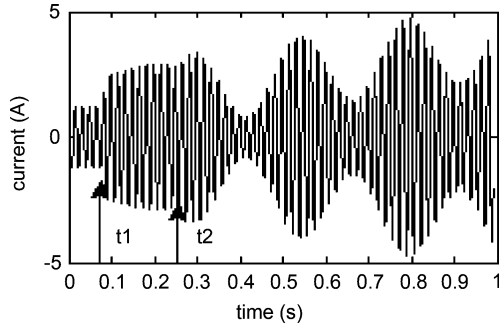

Fig. 14. Current waveform under the out-of-step condition.

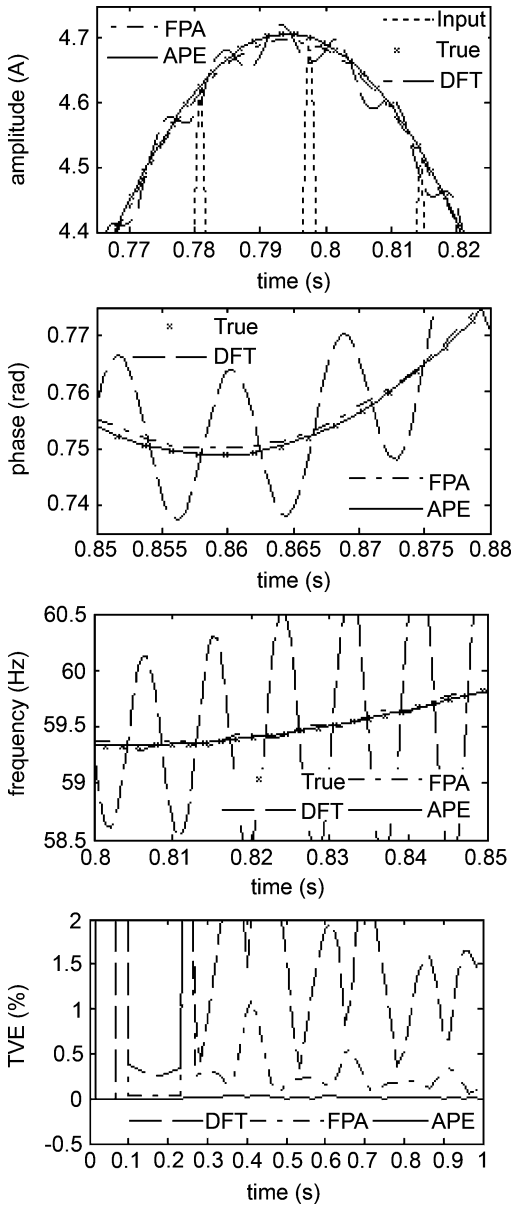

Fig. 15. Estimated amplitude, phase, frequency, and TVE for three algorithms.

results in Fig. 15, we can observe that the adaptive method successfully detected and localized the discontinuous point t_1 and t_2 so that their effects on outputs were eliminated.

VII. Conclusions

An adaptive approach for estimating phasor under power system transient conditions in real-time is proposed in this paper. The conclusions are as follows.

- The wavelet method is able to identify and localize the disturbance while discriminating from various noise within a given data window.
- The effect of electromagnetic transients can be eliminated by using the adaptive data window.
- The quadratic polynomial model achieves better accuracy during power oscillations.
- The proposed approach can be implemented for real-time synchrophasor estimation. It can also be used as the reference algorithm for testing devices performing synchrophasor measurements.
- The proposed algorithm for disturbance detection can be used to indicate the phasor quality so that the power system applications are able to be aware of whether the phasors they use or the results based on the phasors are valid or not.

Appendix

From (16) and (17), we have

$$a(t)\cos[\varphi(t)] = q_0 + q_1 t + q_2 t^2 \tag{24a}$$

$$a(t)\sin[\varphi(t)] = r_0 + r_1 t + r_2 t^2. \tag{24b}$$

For $t = 0$, they are equivalent to $a(0)\cos[\varphi(0)] = q_0$, $a(0)\sin[\varphi(0)] = r_0$. Then, we obtain

$$A_1 = a(0) = (q_0^2 + r_0^2)^{1/2} \varphi_1 = \arctan\left(\frac{r_0}{q_0}\right). \tag{25}$$

Take the first derivative on both sides of (24a) and (24b). For $t = 0$, we have

$$a'(0)\cos[\varphi(0)] - a(0)\varphi'(0)\sin[\varphi(0)] = q_1 \tag{26a}$$

$$a'(0)\sin[\varphi(0)] + a(0)\varphi'(0)\cos[\varphi(0)] = r_1. \tag{26b}$$

Substituting $a(0)\cos[\varphi(0)] = q_0$, $a(0)\sin[\varphi(0)] = r_0$, and eliminating $a'(0)$, we obtain

$$\varphi'(0) = \frac{q_0 r_1 - r_0 q_1}{q_0^2 + r_0^2}. \tag{27}$$

References

[1] North American Electric Reliability Corporation, Real-Time Application of Synchrophasors for Improving Reliability, Oct. 18, 2010. [Online]. Available: http://www.nerc.com/docs/oc/rapirtf/RAPIR%20final%20101710.pdf.

[2] A. Bose, "Smart transmission grid applications and their supporting infrastructure," *IEEE Trans. Smart Grid*, vol. 1, no. 1, pp. 11–19, Jun. 2010.

[3] J. De La Ree, V. Centeno, J. S. Thorp, and A. G. Phadke, "Synchronized phasor measurement applications in power systems," *IEEE Trans. Smart Grid*, vol. 1, no. 1, pp. 20–27, Jun. 2010.

[4] T. L. Baldwin, L. Mili, M. B. Boisen, Jr, and R. Adapa, "Power system observability with minimal phasor measurement placement," *IEEE Trans. Power Syst.*, vol. 8, no. 2, pp. 707–715, May 1993.

[5] S. Chakrabarti and E. Kyriakides, "PMU measurement uncertainty considerations in WLS state estimation," *IEEE Trans. Power Syst.*, vol. 24, no. 2, pp. 1062–1071, May 2009.

[6] J. F. Hauer, W. A. Mittelstadt, K. E. Martin, J. W. Burns, H. Lee, J. W. Pierre, and D. J. Trudnowski, "Use of the WECC WAMS in wide-area probing tests for validation of system performance and modeling," *IEEE Trans. Power Syst.*, vol. 24, no. 1, pp. 250–257, Feb. 2009.

[7] R. Emami and A. Abur, "Robust Measurement design by placing synchronized phasor measurements on network branches," *IEEE Trans. Power Syst.*, vol. 25, no. 1, pp. 38–43, Feb. 2010.

[8] J. Jiang, C. Liu, and C. Chen, "A novel adaptive PMU-based transmission-line relay-design and EMTP simulation results," *IEEE Trans. Power Del.*, vol. 17, no. 4, pp. 930–937, Oct. 2002.

[9] M. G. Adamiak, A. P. Apostolov, M. M. Begovic, C. F. Henville, K. E. Martin, G. L. Michel, A. G. Phadke, and J. S. Thorp, "Wide area Protection—Technology and infrastructures," *IEEE Trans. Power Del.*, vol. 21, no. 2, pp. 601–609, Apr. 2006.

[10] R. Diao, K. Sun, V. Vittal, R. J. O'Keefe, M. R. Richardson, N. Bhatt, D. Stradford, and S. K. Sarawgi, "Decision tree-based online voltage security assessment using PMU measurements," *IEEE Trans. Power Syst.*, vol. 24, no. 2, pp. 832–839, May 2009.

[11] S. Corsi and G. N. Taranto, "A real-time voltage instability identification algorithm based on local phasor measurements," *IEEE Trans. Power Syst.*, vol. 23, no. 3, pp. 1271–1279, Aug. 2008.

[12] C. P. Steinmetz, "Complex quantities and their use in electrical engineering," in *Proc. Int. Elect. Congr., AIEE* , Chicago, IL, 1893, pp. 33–74.

[13] *IEEE Standard for Synchrophasors for Power Systems*, IEEE Standard C37.118-2005, Mar. 2006.

[14] A. G. Phadke and J. S. Thorp, *Computer Relaying for Power Systems*. New York: Wiley, 1988.

[15] J. A. de la O. serna and K. E. Martin, "Improving phasor measurements under power system oscillations," *IEEE Trans. Power Syst.*, vol. 18, no. 1, pp. 160–166, Feb. 2003.

[16] J. A. de la O. serna, "Dynamic phasor estimates for power system oscillations," *IEEE Trans. Instrum. Meas.*, vol. 56, no. 5, pp. 1648–1657, Oct. 2007.

[17] W. Premerlani, B. Kasztenny, and M. Adamiak, "Development and implementation of a synchrophasor estimator capable of measurements under dynamic conditions," *IEEE Trans. Power Del.*, vol. 23, no. 1, pp. 109–123, Jan. 2008.

[18] R. K. Mai, Z. Y. He, L. Fu, B. Kirby, and Z. Q. Bo, "A dynamic synchrophasor estimation algorithm for online application," *IEEE Trans. Power Del.*, vol. 25, no. 2, pp. 570–578, Apr. 2010.

[19] A. G. Phadke and B. Kasztenny, "Synchronized phasor and frequency measurement under transient conditions," *IEEE Trans. Power Del.*, vol. 24, no. 1, pp. 89–95, Jan. 2009.

[20] IEEE Power System Relay Committee Working Group D6, "Power swing and out-of-step considerations on transmission lines," Jun. 2005. [Online]. Available: http://www.pes-psrc.org/Reports

[21] S. Mallat and W. L. Hwang, "Singularity detection and processing with wavelets," *IEEE Trans. Inf. Theory*, vol. 38, no. 2, pp. 617–643, Mar. 1992.

[22] Y. Yuan, L. Yang, and J. Liu, "Characterization of Dirac-structure edges with wavelet transform," *IEEE Trans. Syst., Man, Cybern. B, Cybern.*, vol. 30, no. 1, pp. 93–109, Feb. 2000.

[23] J. Canny, "A computational approach to edge detection," *IEEE Trans. Pattern Anal. Mach. Intell.*, vol. PAMI-8, no. 6, pp. 679–698, Nov. 1986.

[24] S. Mallat, *A Wavelet Tour of Signal Processing*, 3rd ed. London, U.K.: Academic Press, 2008.

[25] *IEEE Standard for Synchrophasors for Power Systems*, IEEE Standard C37.118.1-2011, Dec. 2011.

[26] J. Ren, M. Kezunovic, and J. Stenbakken, "Characterizing dynamic behavior of PMUs using step signals," *Eur. Trans. Elect. Power*, Oct. 2010.

[27] Power System Relaying Committee, "EMTP reference models for transmission line relay testing report, draft 10a," 2004. [Online]. Available: http://www.pes-psrc.org

Jinfeng Ren (S'07) received the B.S. degree in electrical engineering from Xi'an Jiaotong University, Xi'an, China, in 2004 and is currently pursuing the Ph.D. degree in electrical engineering at Texas A&M University, College Station.

He continued research in electric power systems until 2006. His research interests are new algorithms and test methodology for synchrophasor measurements and their applications in power system protection and control, as well as new digital signal processing techniques for power system measurement and instrumentation, and automated simulation methods for multifunctional intelligent electronic device testing.

Mladen Kezunovic (S'77–M'80–SM'85–F'99) received the Dipl. Ing. degree in electrical engineering from the University of Sarajevo, Bosnia, in 1974, and the M.S. and Ph.D. degrees in electrical engineering from the University of Kansas, Lawrence, in 1977 and 1980, respectively.

Currently, he is the Eugene E. Webb Professor and Site Director of the Power Engineering Research Center (PSerc), a National Science Foundation I/UCRC.at Texas A&M University, College Station. He was with Westinghouse Electric Corp., Pittsburgh, PA, from 1979 to 1980 and the Energoinvest Company, in Europe from 1980 to 1986, and spent a sabbatical at EdF, Clamart, France, from 1999 to 2000. He was also a Visiting Professor at Washington State University, Pullman, from 1986 to 1987 and The University of Hong Kong in Fall 2007. His main research interests are digital simulators and simulation methods for intelligent electronic device testing as well as the application of intelligent methods to power system monitoring, control, and protection.

Dr. Kezunovic is a Registered Professional Engineer in Texas and a member of CIGRE.